NASA TECHNICAL NOTE

NASA TN D-8485

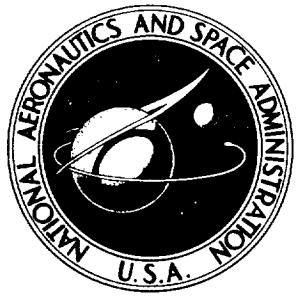

NASA TN D-8485

EXPERIMENTAL EVALUATION OF A BREADBOARD HEAT AND PRODUCT-WATER REMOVAL SYSTEM FOR A SPACE-POWER FUEL CELL DESIGNED WITH STATIC WATER REMOVAL AND EVAPORATIVE COOLING

Norman H. Hagedorn and Paul R. Prokopius

Lewis Research Center
Cleveland, Ohio 44135

NATIONAL AERONAUTICS AND SPACE ADMINISTRATION • WASHINGTON, D. C. • MAY 1977

1. Report No. NASA TN D-8485	2. Government Accession No.	3. Recipient's Catalog No.
4. Title and Subtitle EXPERIMENTAL EVALUATION OF A BREADBOARD HEAT AND PRODUCT-WATER REMOVAL SYSTEM FOR A SPACE-POWER FUEL CELL DESIGNED WITH STATIC WATER REMOVAL AND EVAPORATIVE COOLING		5. Report Date May 1977 6. Performing Organization Code
7. Author(s) Norman H. Hagedorn and Paul R. Prokopius		8. Performing Organization Report No. E-8822 10. Work Unit No. 506-23
9. Performing Organization Name and Address Lewis Research Center National Aeronautics and Space Administration Cleveland, Ohio 44135		11. Contract or Grant No. 13. Type of Report and Period Covered Technical Note
12. Sponsoring Agency Name and Address National Aeronautics and Space Administration Washington, D.C. 20546		14. Sponsoring Agency Code
15. Supplementary Notes		

16. Abstract

A test program was conducted to evaluate the design of a heat and product-water removal system to be used with a fuel cell having static water removal and evaporative cooling. The program, which was conducted on a breadboard version of the system, provided a general assessment of the design in terms of operational integrity and transient stability. This assessment showed that, on the whole, the concept appears to be inherently sound but that in refining this design, several facets will require additional study. These involve interactions between pressure regulators in the pumping loop that occur when they are not correctly matched and the question of whether an ejector is necessary in the system.

17. Key Words (Suggested by Author(s))	18. Distribution Statement
Hydrogen-oxygen fuel cells Spacecraft power supplies	Unclassified - unlimited STAR Category 44

19. Security Classif. (of this report)	20. Security Classif. (of this page)	21. No. of Pages	22. Price*
Unclassified	Unclassified	25	A02

* For sale by the National Technical Information Service, Springfield, Virginia 22161

EXPERIMENTAL EVALUATION OF A BREADBOARD HEAT AND PRODUCT-WATER REMOVAL SYSTEM FOR A SPACE-POWER FUEL CELL DESIGNED WITH STATIC WATER REMOVAL AND EVAPORATIVE COOLING

by Norman H. Hagedorn and Paul R. Prokopius

Lewis Research Center

SUMMARY

The goal of this study was to provide a general assessment of a heat and product-water removal system proposed for a space-power fuel cell having evaporative cooling and static water removal. A program to test transient behavior was conducted in order to provide the data needed to make this evaluation.

The system tested was made up of a breadboard version of the heat and water removal flow network and a simulated fuel-cell module. The fuel-cell simulation was a mathematical-mechanical combination of a computerized model of the thermal and product-water characteristics of the fuel cell and the two steam generation loops. The model was programmed to control the steam loops and thereby to generate, for the breadboard system, the evaporated-coolant and product-water effluent streams of the fuel cell.

The test program provided a general characterization of the transient system response, and from this the basic system design was assessed. The assessment indicated that several areas would require additional study in furthering the proposed design past the breadboard stage. These involve interactions between pressure regulators in the pumping loop that occur when they are not correctly matched and the question of whether an ejector is necessary in the system. However, no basic or inherent problems were discovered, and the system is considered a viable design for the advanced-technology fuel cell.

INTRODUCTION

Hydrogen-oxygen fuel cells have been used for power generation on the Biosatellite, Gemini, and Apollo space missions and will be used on the Space Shuttle. In each in-

stance, the system for removing waste heat and product water from the fuel cells has been tailored to the specific characteristics of the particular fuel cell being used.

Now an advanced fuel cell has been developed that uses "static" water removal and evaporative cooling (ref. 1) techniques not used heretofore on space missions. Until now, no complete system has been evaluated in terms of its ability to manage the heat and water removal from these new fuel cells. However, the developer of the fuel cells has proposed a conceptual design (ref. 1) for such a system. This report presents the results of the first experimental evaluation of a breadboard system based on that design.

The breadboard system did not include a functioning fuel-cell module. Instead, two steam streams, one simulating the product water and the other simulating the evaporated coolant water from a module, were introduced into the system. These streams were controlled by an analog computer model of the thermal characteristics of a fuel-cell module (fig. 1). Power levels over the range of 1.4 to 7 kilowatts were simulated. The system was evaluated in terms of its response to step changes in the power level of the simulated fuel-cell module.

SYMBOLS

A	total area in module of the electrodes or oxygen/coolant plates, 5.56 m^2
a	constant, 332.8 K; 139.2° F
b	constant, 4.37×10^{-4} K/(N/m^2); 5.43° F/psia
C_p	module heat capacity, 1174 J/(kg)(°C); 0.281 Btu/(lbm)(°F)
d	oxygen/coolant plate thickness, 7.62×10^{-4} m; 0.03 in.
F	Faraday's constant, 96 500 C/equivalent
ΔH_{fg}	latent heat of vaporization of water, 2.32×10^{6} J/kg; 1000 Btu/lbm
k	effective thermal conductivity of oxygen/coolant plate, 0.173 J/(m)(sec)(K); 1.2 Btu-in./(hr)(ft^2)(°F)
m	module mass, 28.6 kg; 63.1 lbm
n	number of electrons transferred
P_e	evaporator pressure, N/m^2
P_{eo}	pressure upstream of evaporator orifice, N/m^2
P_t	net electrical output of module, kW
Q_p	rate of heat leaving module as latent heat of vaporization of product water, J/sec
Q_t	total heat generation rate of module, J/sec

T_e evaporator temperature, K

T_s module temperature, K

t time, sec

$\dot{w}$ flow rate of evaporated coolant, kg/sec

$\dot{w}_{pw}$ flow rate of product water, kg/sec

τ time constant

Subscripts:

ss steady state

0 initial

FUEL CELL

A cross-sectional view of a fuel cell with static product-water removal and evaporative cooling is shown in figure 2. The innermost structure is an asbestos mat containing aqueous potassium hydroxide electrolyte. Adjacent to each side of the mat is a catalyzed screen electrode. In contact with the hydrogen-side electrode (anode) is a porous plate that serves as an electrolyte reservoir and absorbs changes in electrolyte volume. Shown above the reservoir, but separated from it, is another electrolyte-filled asbestos mat. Product water is removed from the fuel cell by applying a partial vacuum to the chamber above this mat. The partial vacuum causes the electrolyte in this mat to be more concentrated than the electrolyte in the reservoir plate. Water thus evaporates from the reservoir, condenses into the upper mat, and then reevaporates into the vacuum cavity. By selecting the proper reduced pressure to be used, the electrolyte concentration in the reservoir can be held within acceptable limits. This, then, is the static product-water removal concept.

In contact with the oxygen electrode (cathode) is a plate with a flow field machined in each side. Shown next to the lower side of this plate is a semipermeable membrane. Oxygen is introduced adjacent to the oxygen electrode, and liquid water is supplied between the plate and the membrane. Heat from the fuel-cell reaction is conducted through the plate, causing vaporization of the water. The water vapor then passes through the membrane and into a vacuum chamber below the membrane. By controlling the pressure in this vacuum chamber (i.e., the pressure at which the water is permitted to evaporate), the fuel-cell temperature can be held near the desired value.

In a multicell module of fuel cells of this description, the vacuum chambers for product-water removal and evaporative cooling would feed to common manifolds. It would be the function of the system associated with such a module to control and main-

tain the correct vacuum levels in these respective manifolds and to condense, store, and return liquid water to the module as required.

SYSTEM CONCEPT

A schematic (ref. 1) of the system concept suggested by the developer of the advanced fuel cells described in the preceding section is shown in figure 3. The prime mover in this system is a gas-driven diaphragm pump (1).[1] Incoming hydrogen, which is supplied on demand according to the operating power level of the fuel-cell module (2), is the actuating gas. Therefore, the pump speed is a function of module power.

To generate the partial vacuum levels required for product-water and evaporated-coolant (water) removal, the pump recirculates condensate through an ejector (3) situated downstream of the condenser (4). The reduced pressure at the ejector secondary flow inlet induces the flow of the mixture of product-water vapor and evaporated coolant from the fuel-cell module to the condenser, where it is condensed and subcooled. The product-water pressure controller (5) regulates the ejector primary flow rate. The feedback for this controller is a pressure signal from the product-water vapor manifold. The ejector thus removes condensate from the condenser at the rate necessary to hold the product-water vapor pressure (the lowest-pressure point in the system) at its prescribed value. In this way the fuel-cell electrolyte concentration is controlled.

Fuel-cell temperature control is obtained by using a backpressure regulator (6) in the outlet of the evaporated-coolant manifold. The steam passing through this regulator combines with the product-water vapor and flows to the condenser.

The condenser is cooled at a rate adequate to assure some degree of subcooling of the condensate. This is to lessen the possibility of cavitation at the diaphragm pump inlet. Condenser cooling is therefore controlled by a three-way valve (7) in the coolant inlet line. The valve senses condensate temperature and passes flow through the condenser or bypasses flow around it.

As another means to avoid pump cavitation, a bypass around the pump was provided. A pressure regulator in this line (8) was preset to maintain an adequate net positive suction head at the pump inlet.

The net flow of condensate from the pump is directed toward a pressure regulator (9), which controls the return flow of liquid water into the module coolant cavities. This regulator senses the pressure difference between the liquid water and the evaporated coolant (i.e., across the semipermeable membrane). Water is supplied at a rate sufficient to keep the liquid pressure approximately 6895 N/m^2 (1 psi) greater than the evaporated-coolant pressure. This is to assure that vapor bubbles will be expelled

[1] Numbers in parentheses correspond to the numbered components in figures 3 and 4.

through the membrane into the steam cavity. The remainder of the condensate, which represents the product water generated by the module, passes to storage.

The system contains an overboard vent in case of pump or condenser failure or operation of the module at above-design power levels. A backpressure regulator (10) in the vent line senses the product-water vapor pressure. A rise in this pressure will initiate venting. Under this condition, cooling of the module is maintained by water flowing from storage to the module coolant cavities.

BREADBOARD SYSTEM

The original configuration of the breadboard system is shown schematically in figure 4. Hydraulically actuated valves (1, 2) were used to control the flow rates into the system of the two steam streams simulating the product-water flow and the evaporated coolant flow, respectively, from a fuel-cell module. Another hydraulic valve (3) controlled the removal from the system of liquid water, representing the return flow of coolant to the module.

The condenser (4) had a multilayered configuration, with coolant flowing in alternate layers. Fins projected into the flow passages. The heat transfer area on the steam side, including fins, was approximately 0.214 square meter (2.3 ft^2).

Hot and cold utility water were mixed to give a condenser coolant of the desired temperature. An electropneumatic flow controller (5) located in the hot water line, and sensing the mixture temperature, provided control. A similar controller (6) in the mixture line regulated coolant flow to the condenser, thus controlling the condensate temperature.

Two diaphragm pumps (7) driven by a single electric motor, and operating 180^o out of phase with one another, were connected in parallel to simulate the gas-driven diaphragm pump of the conceptual system. Pump speed and stroke were both adjustable.

The ejector (8) downstream of the condenser was specially designed to meet the flow rate and pressure requirements of the system.

The two backpressure regulators (9, 10) for controlling the evaporated-coolant manifold pressure and the overboard vent, respectively, were standard commercial gas utility regulators. They were chosen for their low deadband and good droop characteristics. The two regulators were sized to pass 100 and 220 m^3/hr (3500 and 7700 ft^3/hr), respectively, for a pressure drop of 34 450 N/m^2 (5 psi) with a pressure droop of 249 N/m^2 (1 in. water column). The remaining pressure regulators (11, 12, 13) in the system were commercial types, modified in some cases to meet specific requirements. These modifications consisted of blocking the downstream pressure-sensing port and of tapping through the body below the diaphragm for feedback of pressure from a control point.

Rotameters were used to monitor the flow rates of condensate from the condenser, the condenser coolant, the liquid water leaving the system, and the ejector primary fluid. The rotameters were sized to give a midrange reading at the respective expected nominal flow rates and had an accuracy of ±3 percent of full scale.

Thermocouples were located in the steam inlet lines, at the condenser inlet and outlet, in the condenser coolant inlet and outlet lines, and at the pump inlet.

Pressure transducers were placed in the two steam lines, at the condenser outlet, at the ejector primary inlet, at the diaphragm pump inlet and outlet, and downstream of the hydraulic valve that controlled the exit rate of liquid water from the system. These transducers had a natural frequency of 5000 hertz and a nonlinearity/hysteresis characteristic of ±0.75 percent.

Thermocouple and transducer data were recorded on high-response strip-chart recorders. The recorders exhibit a 90-percent-of-full-scale response rise time of 4 milliseconds and a frequency response characteristic that is flat to 60 hertz.

In general, all instrumentation and control components peripheral to the actual system simulation had response characteristics that were orders-of-magnitude faster than the fastest recorded system response.

EXPERIMENTAL PROCEDURE

Flow Rate Control

To simulate the product-water vapor and evaporated coolant being ejected by an operating fuel cell, it was first necessary to derive a mathematical model of the thermal characteristics of a cell module. This model took the form of a lumped-parameter formulation for the first law of thermodynamics, making the module temperature independent of spatial coordinates. When programmed on an analog computer and subjected to a step forcing in heat generation rate (power level), the model calculated and controlled the flow rates of product-water vapor and evaporated coolant water into the system (fig. 5). Feedback from the system of the evaporated-coolant pressure permitted continuous calculation of the simulated-module temperature (see appendix A for the derivation and use of the thermal model).

The steam, which was introduced into the system in two streams, was generated in an electrically heated boiler. It was superheated by in-line heaters to prevent condensation of the streams before they reached the condenser. By trial and error it was determined how much superheat to add to just balance the heat loss between the system inlets and the condenser.

Closed-loop controllers were used to actuate hydraulic valves that regulated the upstream steam pressure on (i.e., the flow rate through) choked orifices at the inlets

to the system. The computer calculated the flow-rate set points, and the feedbacks were the pressures measured upstream of the orifices.

As an example, the signal $T_s - T_e$ (see SYMBOLS section) was used as the set point for the evaporated-coolant flow controller. The orifice calibration $\dot{w} = f(P_{eo})$, where P_{eo} is the pressure upstream of the evaporator orifice, and the relation $\dot{w}\,\Delta H_{fg} = kA(T_s - T_e)/d$ were used for computer conversion of the feedback pressure signal into the same form as that of the set point: $(T_s - T_e) = f(P_{eo})\,\Delta H_{fg} d/kA$. The difference, $(T_s - T_e)_{setpoint} - (T_s - T_e)_{feedback}$, provided the actuating signal for the flow controller. A similar approach was taken for controlling the flow rates of product water into, and liquid water out of, the system.

System Modifications

Early in the experimental program, it was decided to make several changes in the breadboard system. Although these changes represented deviations from the original concept, it was felt that they would not have a profound effect on the conclusions to be reached.

First, the overboard vent provision in the system was eliminated because it was not possible to make that portion of the system adequately leak free and the in-leakage of air was causing operational difficulties. Since the test program did not call for simulation of any conditions that would lead to overboard venting, it was felt that this deletion was reasonable.

Next, it was found that the method used to control the condensate temperature was inherently unstable. The instability was a function of the condenser orientation, the feedback thermocouple location, the magnitude of the simulated change in power level, the coolant flow controller gains, and the pressure variations in the system. Several modifications were made in the condenser coolant subsystem with little, if any, improvement in performance. Finally, it was decided simply to use cold utility water as the condenser coolant. The flow rate was set constant at a high enough value to handle the maximum heat load to be introduced to the condenser. The condensate temperature was thus permitted to drift during the course of the experiments.

Finally, for the sake of simplicity, it was decided not to attempt to vary the diaphragm pump speed as a function of simulated power level. If the pump speed had been varied, the only effect would have been to cause the pump inlet pressure regulator and the product-water pressure controller to readjust in order to maintain the proper flow rate through the ejector.

Data Collection

In conducting the experimental program, no attempt was made to map the operation of the system or to do a complete transient analysis. Instead, selected transients were run to obtain data from which the transient characteristics of the system could be determined.

Rapid changes in power demand typify the power profile of space-power fuel cell systems. These demand variations, which ultimately are step changes, represent the primary transient conditions for which the system must be designed. In keeping with this, the breadboard system was studied in terms of its response to step changes in simulated system load power. In determining the general transient characteristics, tests were run with the system parameters set at or near "baseline" conditions and also with variations from baseline. For example, transients were run for a range of diaphragm pump inlet pressures to determine the effect this operating parameter has on the system response.

Over the duration of each transient test, strip-chart recordings were made of 12 key system parameters. These parameters are as follows:

(1) System load power, simulated by a voltage input function to the fuel-cell computer model

(2) Evaporated-coolant flow, recorded as the pressure upstream of a sonic flow-control orifice in the evaporated-coolant flow simulator

(3) Product-water flow, recorded as the steam pressure upstream of a sonic flow-control orifice in the product-water simulator loop

(4) Fuel-cell-module temperature, calculated by the module model

(5) Calculated module-to-evaporator temperature difference, representing the driving force for heat rejection from the module

(6) Evaporator pressure, measured upstream of the evaporated-coolant backpressure regulator

(7) Condenser inlet pressure

(8) Steam temperature measured at the condenser inlet

(9) Condensate temperature, measured at the condenser outlet plenum

(10) Condenser coolant outlet temperature

(11) Ejector primary pressure

(12) Ejector secondary pressure

RESULTS AND DISCUSSION

A sample 1.4- to 7-kilowatt load step transient is shown in figure 6. Figure 6(a) shows the action of the computer simulation, 6(b) the recorded pressure parameter

responses, and 6(c) the recorded temperature responses.

Activated by the load transient shown in figure 6(a), the product-water response generator of the computer model introduced a first-order transient to the product-water flow control. The ensuing flow transient that was generated shows a rise from an initial value of 0.54 kg/hr (1.2 lbm/hr) to a new steady-state value of 2.58 kg/hr (5.7 lbm/hr). Similarly, the computer simulation calculated the illustrated lag responses in T_s and $T_s - T_e$ and, with these data, generated the corresponding evaporated-coolant flow response. The latter, also a first-order response, rises from an initial flow of 0.86 kg/hr (1.9 lbm/hr) to a final value of 5.05 kg/hr (11.1 lbm/hr). The two flow transients generated by the computer-controller simulation of the fuel-cell module represent the perturbation that must be acted on by the heat and water removal system.

The system pressure response transients recorded for the 1.4- to 7-kilowatt load step are shown in figure 6(b). The evaporator pressure, because of the control action of the evaporated-coolant backpressure regulator, shows only a small transient deviation from its set-point value of 51 675 N/m^2 (7.5 psia). On the other hand, the condenser inlet pressure exhibits a transient with a significant overshoot. This suggests the presence of a system response characteristic that is second order or higher. This transient (specifically, the magnitude of the overshoot) is particularly significant in regard to maintaining condenser stability since the condensing interface position is pressure related.

The second-order (overshoot) transient characteristic was thought to be the result of an interaction between the product-water pressure controller in the ejector primary loop and the transient characteristics of the condenser portion of the loop. To determine whether this was, in fact, the situation that existed, subsequent tests were run with the product-water pressure controller blocked in a fixed position. The overshoot characteristic persisted throughout these tests, and thus it could be concluded that the system itself is inherently second order or higher.

As seen in the fourth data trace of figure 6(b), except for an initial 5-second dead time, the condenser pressure transient is transmitted to the secondary port of the ejector. However, it is greatly amplified in the ejector primary loop. This is due to the control action of the ejector loop regulators in response to the condenser inlet transient.

Temperatures in the condenser portion of the loop that were generated by the load step are shown in figure 6(c). The steam temperature at the condenser inlet exhibits an overdamped response with a slow ripple characteristic, and the coolant outlet temperature is an overdamped lag response. The condensate temperature displays a transient characteristic with a 10-second dead time and an overshoot characteristic that coincides with the peak values of the condenser inlet and ejector pressure transients.

In assessing the stability characteristic of the system, transient tests (load steps) were run under a variety of conditions. The effects that were studied included variations

in operating parameters such as system pressure and temperature as well as variations in system control functions. In every case the system was found to perform stably and the data exhibited the basic characteristics that were outlined in figure 6. The closest any test came to generating an unstable situation was one in which all the system parameters were set at or near design conditions, but the nominal ejector primary pressure was 67 520 N/m^2 (9.8 psia) or less (instead of near 70 960 N/m^2 (10.3 psia)). This was accomplished by lowering the set point for the pump inlet pressure regulator. Under these conditions a low-amplitude stable oscillation was observed in the ejector primary and secondary pressures, as well as in the condenser inlet pressure. As the primary pressure was decreased further, the oscillations persisted, and the amplitude remained constant at a relatively small value (5510 N/m^2 (0.8 psi) peak to peak in the ejector primary pressure). These data are presented in figure 7. The fact that the amplitude of the oscillations observed in the ejector primary pressure is attenuated in the condenser portion of the system suggests that the oscillatory characteristic is generated in the pump loop. A possible explanation is that at the lower pressures the ejector loop regulators are closed to the point where their high sensitivities or hysteresis characteristics are sufficient to establish and maintain a stable oscillation.

The ejector was included in the loop design to lessen the possibility of cavitation in the diaphragm pump by providing a positive pumping head to the pump inlet. The ejector also provided some isolation for the fuel-cell module and the condenser from the pressure pulsations of the diaphragm pump. The need for the ejector was somewhat in doubt, so tests were conducted to determine if this requirement was justified. For these tests the product-water pressure controller was moved to a point between the condenser and the diaphragm pump, and the ejector was eliminated from the loop. Various step transients were run with the system configured in this manner without any observable detrimental effects on loop operation. Actually, the system responded better, in that the magnitude of the overshoot characteristic of the condenser inlet pressure response was considerably less than with the ejector installed. A sample load step transient from 1.4 to 7 kilowatts is shown in figure 8. In this case the condenser pressure overshot its final value by 2070 N/m^2 (0.3 psi). For a similar load transient with the ejector active (fig. 6(b)), an overshoot of 5510 N/m^2 (0.8 psi) occurred. The tighter response and control characteristic of this system was not totally unexpected since in this case the controller and the primary vacuum source are more closely coupled to the parameter being regulated. Also, the pulsating action of the diaphragm pump appeared to be beneficial to the controlling action of the system because the evaporated-coolant and product-water regulators were kept in a dynamic state. Thus, any control discontinuity or dead time brought about by regulator friction, or "stiction," was eliminated. In some instances with the ejector installed in the loop, stiction in the evaporated-coolant regulator was indeed observed. An example of this is given in figure 9. This

effect is shown as an uncontrolled buildup in evaporated-coolant pressure for a short time immediately following the load transient. When the control signal magnitude reaches a value that overcomes the stiction, the regulator breaks free and a rapid correction occurs that brings the evaporated-coolant pressure into control. This temporary loss of control and correction for the ensuing nonlinearity is reflected in the system pressure recordings shown in figure 9. In all cases tested with the ejector removed, these effects were not present. As previously stated, without the isolating effects of the ejector, the pulsating pressure of the diaphragm pump can be transmitted back to the system to keep the controllers in continuous action. Considering the fact that without the ejector the system is more responsive and also that any component friction effects might be eliminated, it would appear to be advantageous to eliminate the ejector from the system design. For a complete assessment of this, further study is required.

Since the response characteristics of the fuel-cell product water rejection are not generated by a mass transport model but are approximated by assumption, the influence that this transient has on the overall system response was tested. This was done by varying the time constant of the assumed first-order lag response in product-water flow. The condenser inlet pressure and evaporated-coolant flow are the system parameters used to illustrate these effects. Response transients are shown in figure 10 for 1.4- to 7-kilowatt load steps with the product-water time constant set at 26.5 seconds, the value that was used throughout the test program, plus two variations from this - zero and 53 seconds. In comparing the three transients, some interesting effects were observed. The slowest product-water flow transient 2τ coincides with the fastest of the three evaporated-coolant flow and condenser inlet pressure transients. This can be attributed to the fact that a decrease in the response rate of product-water flow carries with it a decrease in the rate at which heat is being removed from the cell by the product water. To maintain control of the cell temperature, this heat flow rate decrease must be compensated for by an increase in the amount of heat being removed by the evaporator. Therefore, even though product water is being removed at a slower rate, the increased demand placed on the evaporator is apparently the overriding effect and is reflected into the condenser inlet pressure as a higher overshoot characteristic, quicker response, and quicker settling time.

Various tests that were conducted indicate that one portion of the loop that is somewhat design sensitive to a breakdown in system integrity (loss of control) is that portion which includes the ejector and its associated control elements. This loss of control can be caused by a sudden decrease in power and is a result of the second-order (or higher) response characteristic of the condensing portion of the system. Following a step down in power, the pressure in the condenser portion of the loop undergoes an underdamped decrease before steady operation at the set-point pressure is reestablished. Since this pressure serves as the feedback control signal for the product-water pressure controller of the ejector loop, it follows that the pressure decrease can generate an overcor-

rective decrease in the pumping action of the ejector. Contingent on the magnitude of the underdamped decrease, the overcorrection in control could call for a complete shutdown of the product-water pressure controller and hence the primary or pumping stream of the ejector. With this, the control action of the ejector loop is lost and the condenser is exposed to the diaphragm pump vacuum (from the downstream side of the ejector primary through the secondary). In the normal mode of operation, in which the diaphragm pump vacuum is significantly lower than the vacuum being maintained in the condenser, this loss of control would be only momentary. In this situation, control recovery would occur because, with the shutdown of the ejector primary flow, the condenser would suddenly experience the lower vacuum (i.e., higher pressure) of the diaphragm pump inlet. This vacuum decrease would be transmitted to the product-water pressure controller, which would, in turn, reopen and allow the ejector stream to flow and reestablish control of the condenser inlet pressure.

This situation could, however, result in a permanent loss of control if the vacuum being held at the diaphragm pump inlet were high enough to assume control of the condensing portion of the loop. In this case the diaphragm pump would, in effect, eliminate the ejector from the system and the condenser vacuum would not undergo the decrease necessary to reestablish control. The permanent control-loss situation would obviously have a low probability of occurrence because it requires a double contingency in operation, the combination of a response magnitude large enough to cause the product-water pressure controller to shut down and too high a vacuum at the inlet of the diaphragm pump. However, because of the seriousness of a total loss of control, the slightest possibility that this combination could occur must of necessity be considered in any system design.

CONCLUDING REMARKS

From the results of the transient test program, it can be concluded that the system does not display any general tendency toward instability or operational discontinuity. Further, while in the nominal operating range, all the system transients have the general characteristics of slow first-order lags or underdamped second-order (or higher) responses. With one exception, these pose no problems in maintaining control. The one exception is in the ejector loop in which the product-water pressure controller upstream of the ejector can be driven completely closed, while responding to a decrease in load, because of the underdamped characteristic of the condenser loop pressure. Under normal operating conditions this can produce only a momentary interruption in control and with proper design this condition can be eliminated. At an off-design operating condition in which the vacuum being held at the diaphragm pump inlet is large enough to

assume control, this situation can generate a permanent loss of control by the ejector loop. In another off-design condition, in which the product-water pressure controller is nearly closed, an oscillation is established in the ejector and condenser portions of the system. Neither this nor the ejector control loss situation could be considered to be a problem inherent in the system concept. However, in any further design or prototype testing these situations would warrant additional analyses to assess, and ultimately guard against, their probability of occurring.

Also worthy of some additional investigation would be an assessment of the value of the ejector to the system design. Tests in this program showed that the system could be made to operate without the ejector, and in some respects performance was improved. However, a complete assessment of the basic system design characteristics, such as stability or controllability, was not conducted.

On the whole the performance of the breadboard was considered to be acceptable. Based on this and the fact that a good deal of care was taken in making the breadboard a credible representation of the proposed system, the configuration tested is considered a viable design for the advanced-technology fuel cell.

Lewis Research Center,
National Aeronautics and Space Administration,
Cleveland, Ohio, January 14, 1977,
506-23.

APPENDIX A

DERIVATION AND USE OF THE FUEL-CELL-MODULE THERMAL MODEL

According to the first law of thermodynamics, (Rate of heat accumulation) = (Rate of heat generation) - (Rate of heat loss), or (see SYMBOLS section)

$$mC_p \frac{dT_s}{dt} = Q_t - \dot{w}_{pw} \Delta H_{fg} - \frac{kA(T_s - T_e)}{d} \tag{1}$$

Rewriting yields

$$\dot{T}_s + \frac{kA}{dmC_p} T_s = \frac{Q_t}{mC_p} - \frac{\dot{w}_{pw} \Delta H_{fg}}{mC_p} + \frac{kA}{mC_p d} T_e \tag{2}$$

The first term on the right side of equation (1) represents the total heat generation rate of the module. Step changes in this parameter provided the forcing for the model.

The second term corresponds to the heat leaving the module as latent heat of vaporization of the product water. In reality, this term is a function of module temperature, electrolyte concentration, product-water cavity pressure, time, etc. Because there was insufficient computer capacity for an exact representation of this function, it was approximated by an exponential term as follows: letting $Q_p = \dot{w}_{pw} \Delta H_{fg}$ and using a polarization curve for a typical fuel cell in a module, it is possible to calculate Q_t and a steady-state value for $Q_p \equiv Q_{p_{ss}}$ (see appendix B for typical derivations). For any power level, then, the ratio $\left(Q_{p_{ss}}/Q_t\right)$ is known. Therefore, before a step change was introduced in Q_t, a potentiometer in the analog computer was set to the value of $Q_{p_{ss}}/Q_t$ that corresponded to the steady-state heat rates at the new power level. When the step change was introduced, the computer-calculated difference $Q_t\left(Q_{p_{ss}}/Q_t\right) - Q_{p_0}$ was fed into a first-order lag generator. The signal thus generated by the computer was

$$\dot{w}_{pw} \Delta H_{fg} = Q_p(t) = Q_{p_0} + \left(Q_{p_{ss}} - Q_{p_0}\right)\left(1 - e^{-t/\tau}\right) \tag{3}$$

where Q_{p_0} represents the initial condition. The time constant τ was treated as an experimental parameter.

Returning to equation (1), the final term on the right side contains the temperature at which coolant water vaporizes into the steam manifold. This temperature is the

feedback from the breadboard system to the analog model. However, the parameter actually measured in the breadboard system was the steam manifold pressure. To convert this pressure into an equivalent temperature, the vapor-pressure-against-temperature curve for water was linearized over a small temperature range centered at the nominal temperature for the steam manifold, 355.4 K (180° F). The computer was then programmed to calculate $T_e = a + bP_e$, where P_e is the measured steam manifold pressure and a and b are the intercept and slope of the linearized curve.

It was recognized that the possibility existed for the calculated instantaneous module temperature to be lower than the steam manifold temperature (e.g., if the manifold pressure were to rise for some reason). The model would then imply that heat was flowing back into the module. To avoid this anomaly, the signal $T_s - T_e$ was fed to a comparator. When this temperature difference was negative, the signal was blocked from the computer integrator. Under this condition the model then became

$$\dot{T}_s = \frac{Q_t}{mC_p} - \frac{\dot{w}_{pw}\,\Delta H_{fg}}{mC_p} \tag{4}$$

which states that all the heat being generated is either accumulated in the module or leaves with the product water. When the calculated temperature difference $T_s - T_e$ once again became positive, the model returned to the form given in equation (2).

APPENDIX B

SAMPLE CALCULATIONS

To determine the total heat generation rate Q_t and the heat leaving the module with the product water at steady state $Q_{p_{ss}}$ as functions of total power P_t, consider a fuel-cell module with a total electrode area of 5.56 square meters (60 ft^2) and made up of single cells giving 0.89 volt at 1079 A/m^2 (100 A/ft^2). The thermal efficiency can be derived by first defining a fictitious voltage V_t in terms of the heat of reaction for the reaction $(H_2)_g + \frac{1}{2}(O_2)_g - (H_2O)_l$.

$$V_t = \frac{-\Delta H}{nF} = 1.48 \text{ volts}$$

Then, the thermal efficiency $\eta_t = V/V_t = 0.89/1.48 = 0.60$. Also, η_t = Net power/(Net power + Waste heat) = $P_t/(P_t + Q_t)$, or $Q_t = P_t(1 - \eta_T)/\eta_T$. In this case, P_t = (1079 A/m^2) (5.56 m^2) (0.89 volt) = 5.34 kW. Therefore, Q_t = (5.34)(1 - 0.60)/0.60 = 3.56 kW.

Now, $Q_{p_{ss}} = \dot{w}_{pw} \Delta H_{fg}$. It was assumed that $\Delta H_{fg} = 2.32 \times 10^6$ J/kg (1000 Btu/lbm H_2O) and $\dot{w}_{pw}$ = (0.94×10^{-7} kg H_2O/(A)(sec)) (1079 A/m^2)(5.56 m^2) = 5.64×10^{-4} kg/sec. Thus, $Q_{p_{ss}}$ = (5.64×10^{-4} kg/sec)(2.32×10^6 J/kg) = 1.31 kW and $(Q_{p_{ss}}/Q_t)$ = 1.31/3.56 = 0.368.

By using other values of current density and obtaining corresponding single-cell voltages from a polarization curve, repetition of these calculations permitted curves of Q_t and $(Q_{p_{ss}}/Q_t)$ against P_t to be drawn.

REFERENCE

1. Grevstad, P. E.: Development of Advanced Fuel Cell System. (PWA-4542, Pratt & Whitney Aircraft; NAS3-15339) NASA CR-121136, 1972.

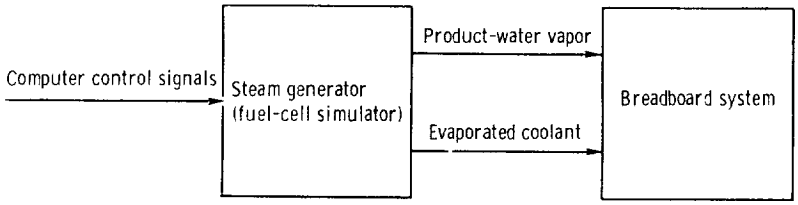

Figure 1. - Fuel-cell-module simulation.

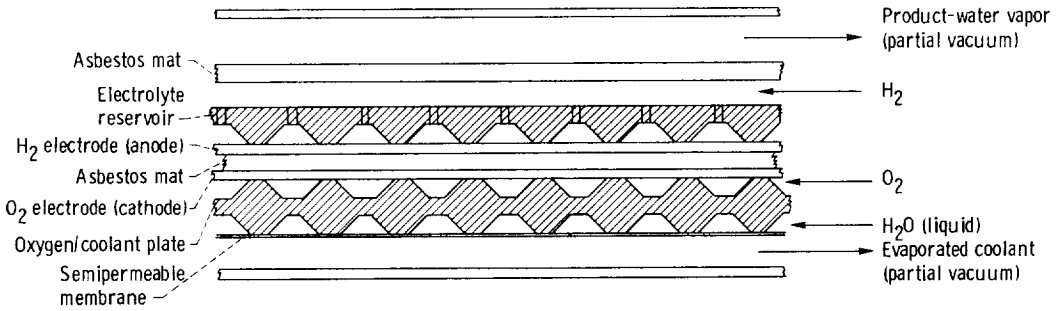

Figure 2. - Fuel cell with static product-water removal and evaporative cooling.

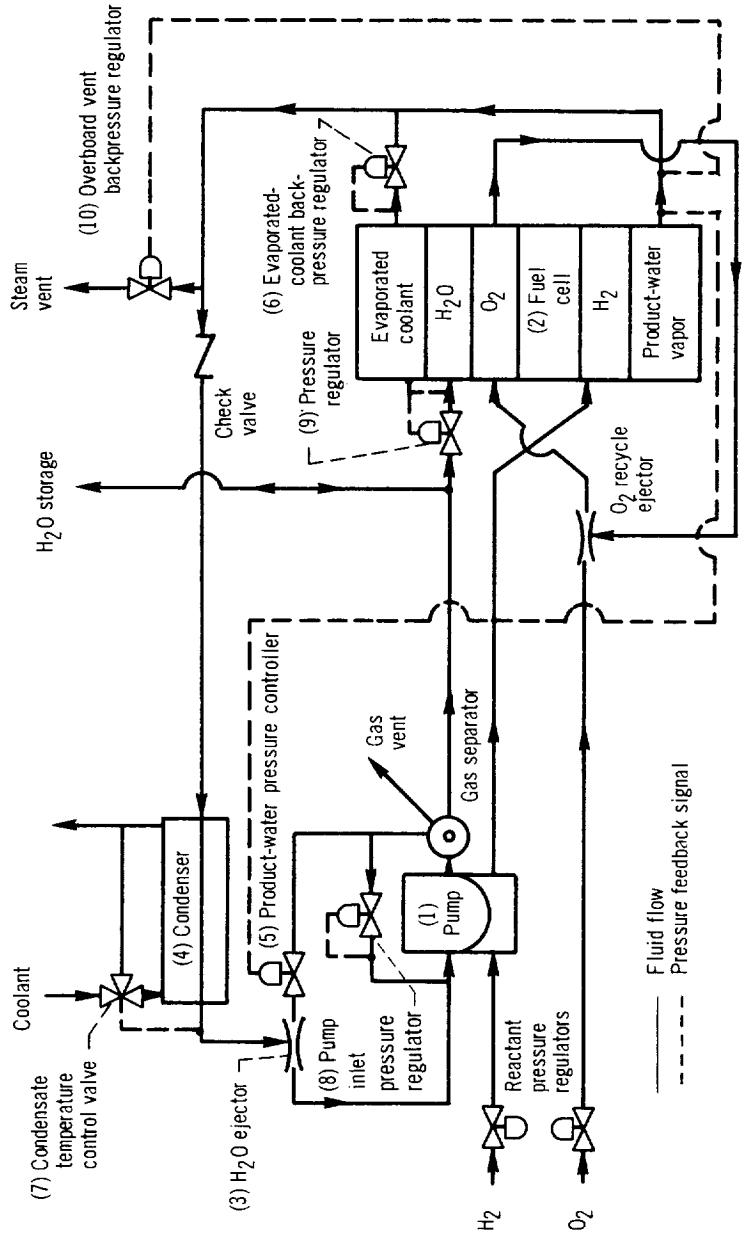

Figure 3. - System concept.

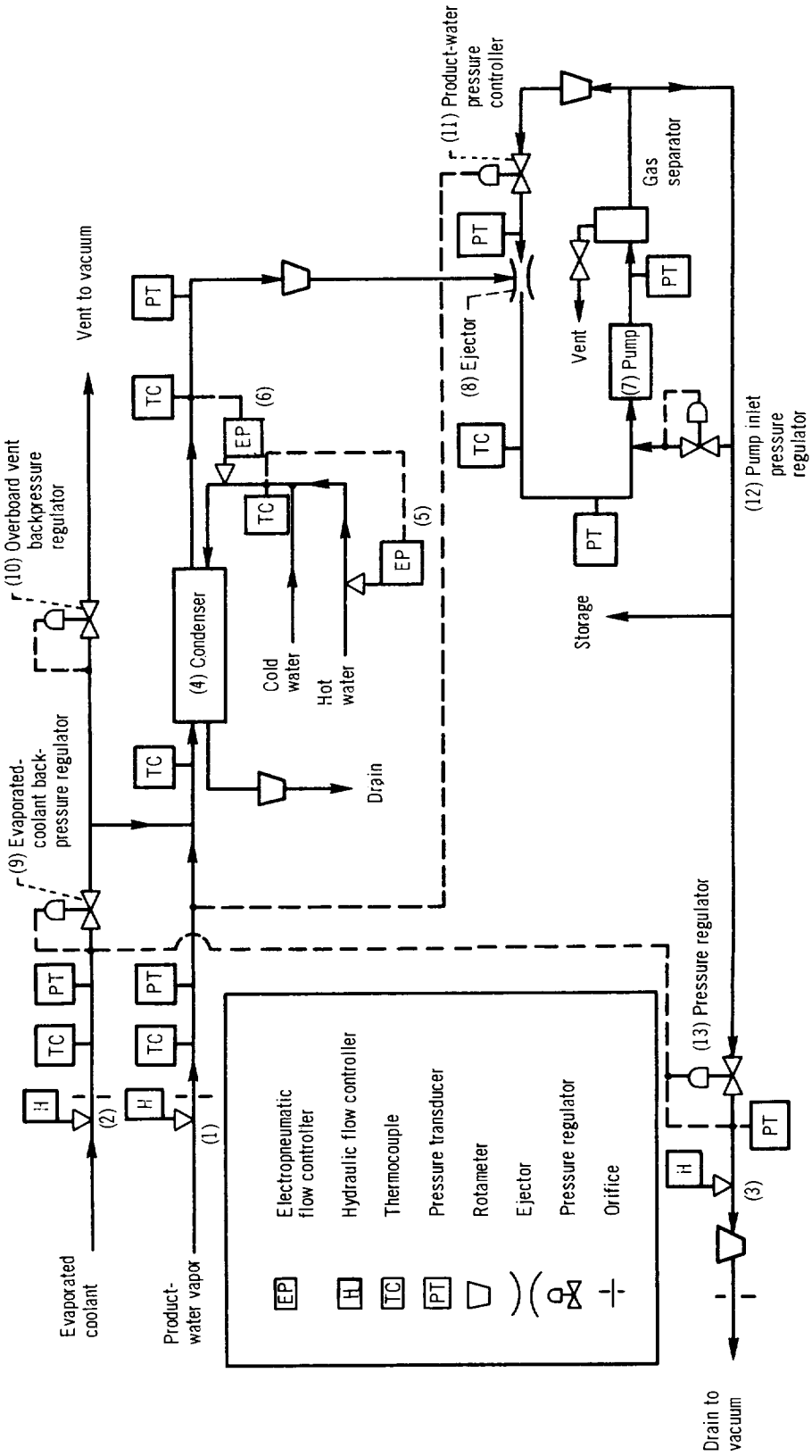

Figure 4. - Schematic of original breadboard system.

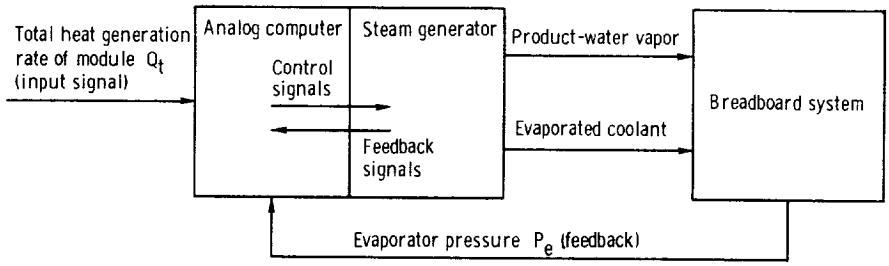

Figure 5. - Signal and fluid flow diagram.

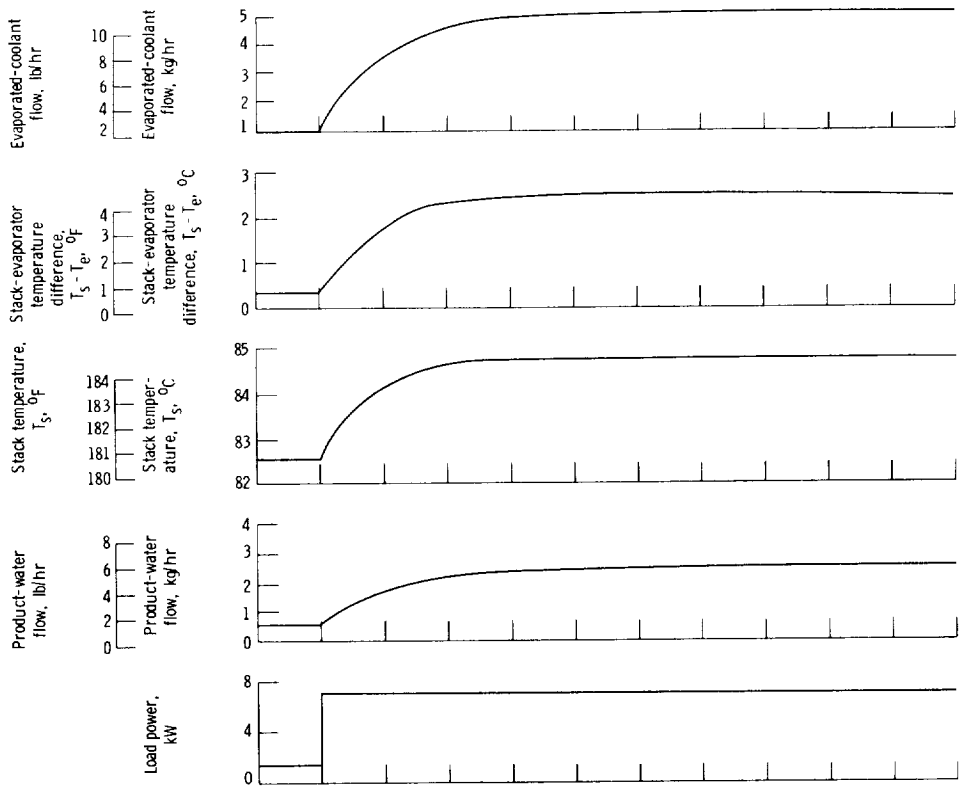

(a) Computer-simulated fuel cell response transients.

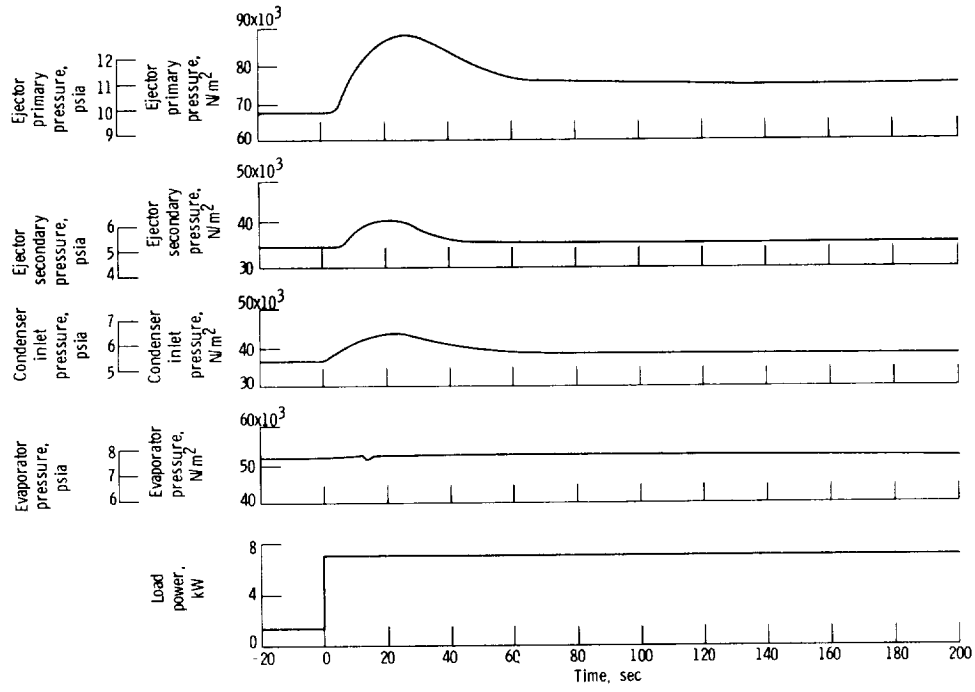

(b) System pressure response transients.

Figure 6. - Response transients for a 1.4- to 7-kilowatt load step.

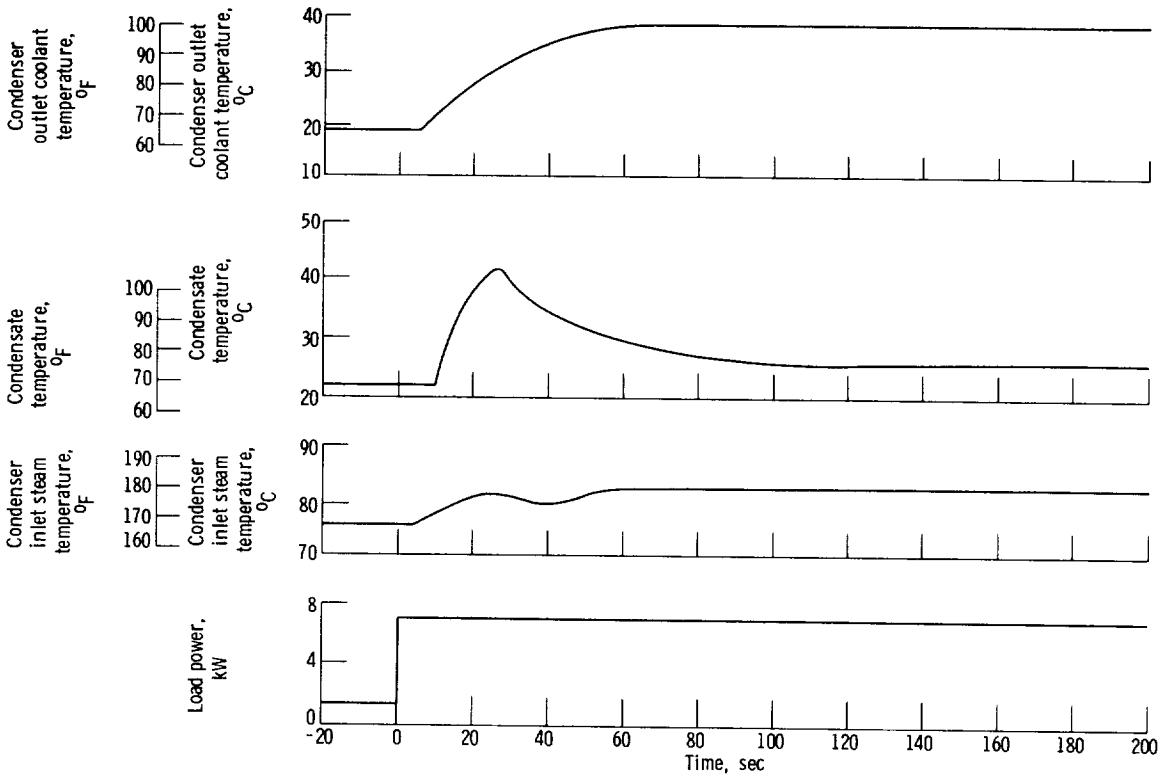

(c) System temperature response transients.

Figure 6. - Concluded.

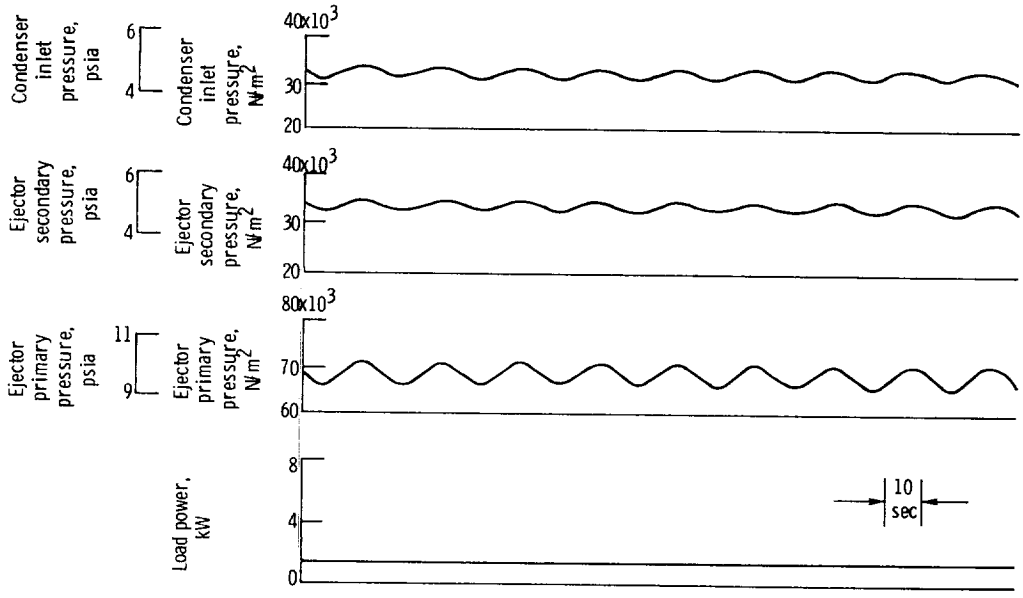

Figure 7. - Stable pressure oscillation of vacuum pump loop.

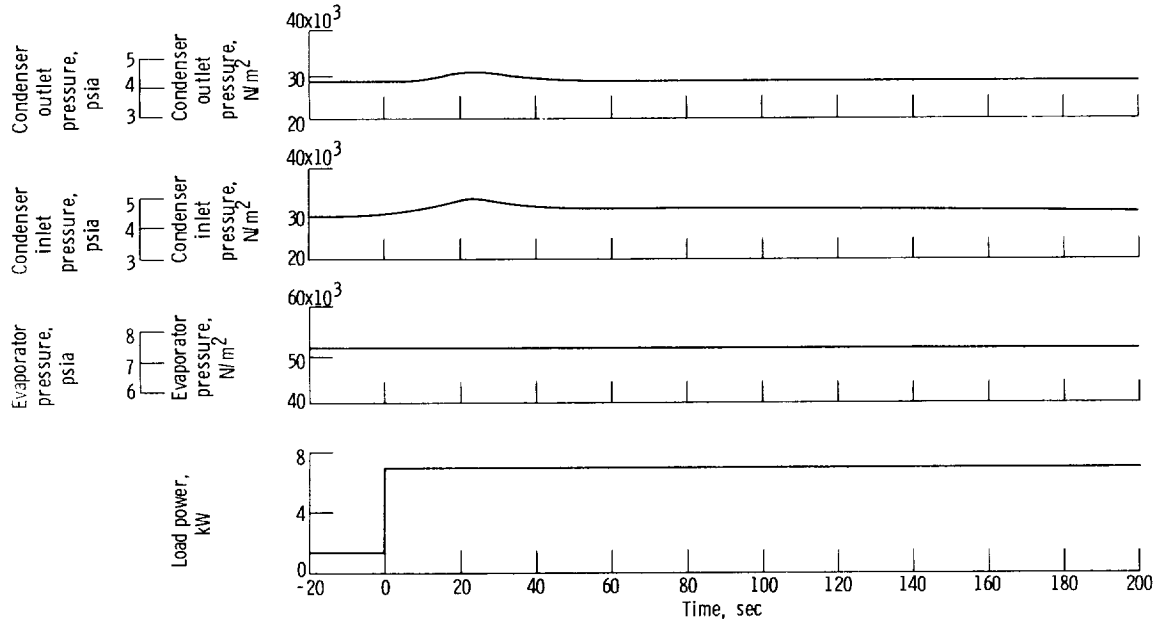

Figure 8. - System pressure transients for a 1.4- to 7-kilowatt load step with ejector removed.

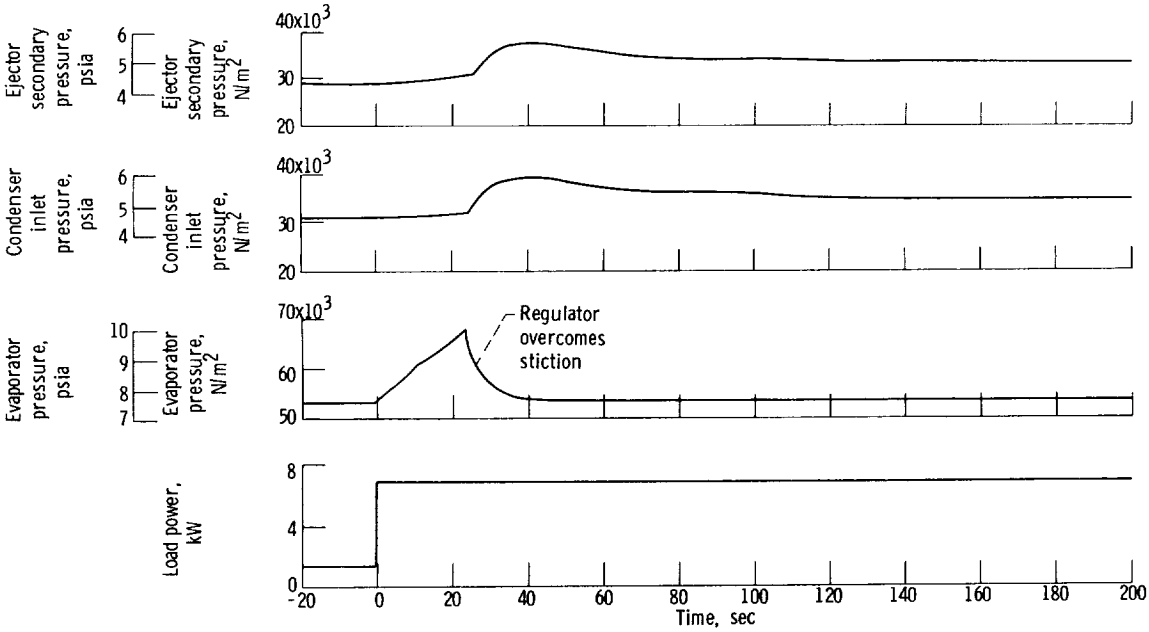

Figure 9. - System pressure response transients for a 1.4- to 7-kilowatt load step with nonlinear regulator action (stiction).

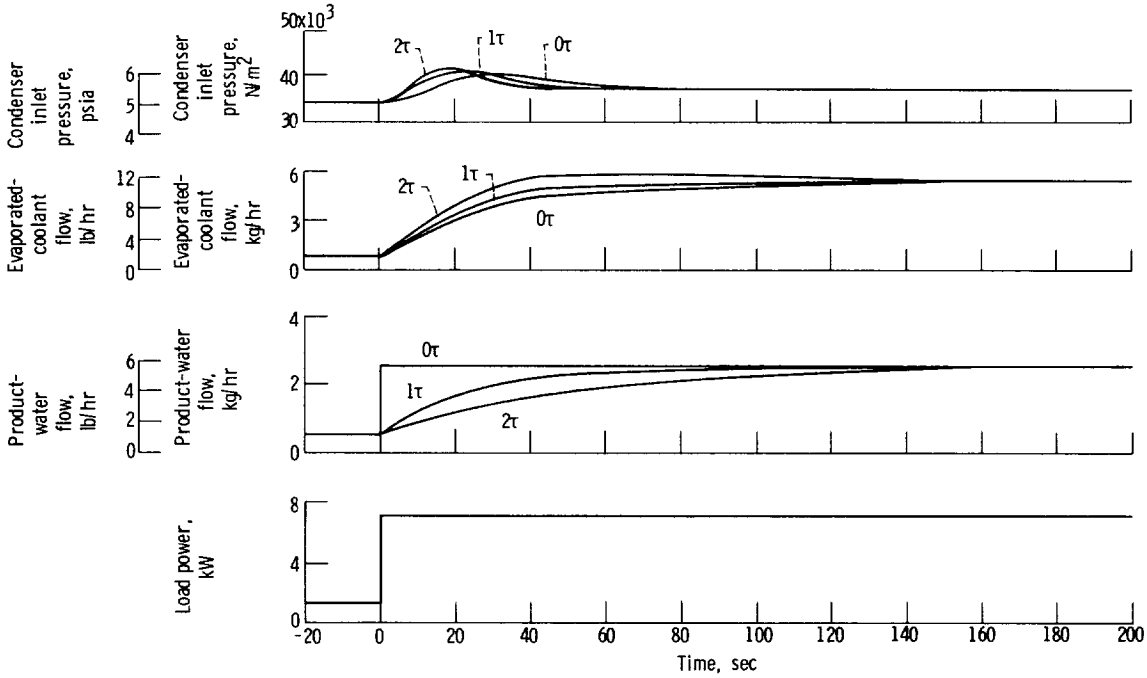

Figure 10. - Influence of product-water response speed on transient characteristics of the other system parameters for 1.4- to 7-kilowatt load step.

"The aeronautical and space activities of the United States shall be conducted so as to contribute . . . to the expansion of human knowledge of phenomena in the atmosphere and space. The Administration shall provide for the widest practicable and appropriate dissemination of information concerning its activities and the results thereof."

—NATIONAL AERONAUTICS AND SPACE ACT OF 1958

NASA SCIENTIFIC AND TECHNICAL PUBLICATIONS

TECHNICAL REPORTS: Scientific and technical information considered important, complete, and a lasting contribution to existing knowledge.

TECHNICAL NOTES: Information less broad in scope but nevertheless of importance as a contribution to existing knowledge.

TECHNICAL MEMORANDUMS: Information receiving limited distribution because of preliminary data, security classification, or other reasons. Also includes conference proceedings with either limited or unlimited distribution.

CONTRACTOR REPORTS: Scientific and technical information generated under a NASA contract or grant and considered an important contribution to existing knowledge.

TECHNICAL TRANSLATIONS: Information published in a foreign language considered to merit NASA distribution in English.

SPECIAL PUBLICATIONS: Information derived from or of value to NASA activities. Publications include final reports of major projects, monographs, data compilations, handbooks, sourcebooks, and special bibliographies.

TECHNOLOGY UTILIZATION PUBLICATIONS: Information on technology used by NASA that may be of particular interest in commercial and other non-aerospace applications. Publications include Tech Briefs, Technology Utilization Reports and Technology Surveys.

Details on the availability of these publications may be obtained from:

SCIENTIFIC AND TECHNICAL INFORMATION OFFICE

NATIONAL AERONAUTICS AND SPACE ADMINISTRATION

Washington, D.C. 20546